EC
Journals.ASM.org

Temporal Behavior of Capsule Enlargement by *Cryptococcus neoformans*

Radames J. B. Cordero,[a]* Aviv Bergman,[b] Arturo Casadevall[a,c]

Department of Microbiology and Immunology,[a] System and Computational Biology,[b] and Department of Medicine,[c] Albert Einstein College of Medicine, Bronx, New York, New York, USA

Microbial capsules are important virulence traits that mediate cell-host interactions and provide protection against host immune defense mechanisms. *Cryptococcus neoformans* is a yeast-like fungus that is capable of synthesizing a complex polysaccharide (PS) capsule that is required for causing disease. Microscopic visualization of capsule enlargement is difficult, because the capsule is a highly hydrated structure with an index of refraction that is very close to that of aqueous medium. In this study, we took advantage of the capsular reaction ("quellung" effect) produced by IgM monoclonal antibody (MAb) 13F1 to increase the refraction index difference between capsule and medium such that we visualized the capsule using differential interference contrast (DIC) microscopy. Time-lapse size measurements allowed us to quantify the growth rate of the capsule relative to that of the cell body. The increase in capsule volume per unit of time was consistent with a logistic variable slope model in which the capsule's final size was proportional to the rate of its growth. The rate of capsule growth (0.3 to 2.5 μm^3/min) was at least 4-fold faster than the rate of cell body growth (0.1 to 0.3 μm^3/min), and there was large cell-to-cell variation in the temporal kinetics of capsule and cellular growth. Previous to the first cellular replication event, both the capsule and cell body enlarged simultaneously, and their differences showed monotonic growth, which was affected only by its rate of volume increase per unit of time. Using these results, we provide an updated model for cryptococcal capsule biogenesis.

Cryptococcus neoformans is a human-pathogenic fungus that has a distinctive capsule, which is a major virulence factor (1, 2). During an infection, *C. neoformans* is quickly stimulated to synthesize a thick polysaccharide (PS) capsule that reaches diameters larger than its cell body size (3). This mechanism of adaptation presents a significant problem to hosts, given the effectiveness of the capsule against immune defense strategies (i.e., phagocytosis and killing by macrophages) (4). The mechanisms involved in capsule growth remain poorly understood, in large part, because there are few tools to study the process of capsular enlargement.

In addition to its central role in fungus-host interaction, synthesis of a micrometer-size capsule (induced under nutrient-limited conditions) must represent both a substantial energy investment and a highly coordinated biosynthetic process. The major PS capsular component is glucuronoxylomannan (GXM), a very large (10^5 to 10^8 g/mol) and negatively charged heteropolymer formed by different repeating units (or structural reported groups [SRG]) (5). In serotype A strains (i.e., *C. neoformans* H99), the predominant SRG is a mannose triad with xylose and glucuronic acid substitutions ($Man_3Xyl_2GlcA_1$). GXM is synthesized intracellularly in the Golgi apparatus and can be exported extracellularly via vesicles (3, 6–8), where it can incorporate on the cell wall surface. Anchoring of capsular GXM appears to involve PS-PS interactions, including cell-wall-derived PSs, such as α-glucans (9) and chitin-derived structures (10).

Capsule synthesis can be induced *in vitro* by growing the cells in various medium conditions, such as nutrient-limited conditions, mannitol, mammalian serum, carbon dioxide, alkaline pH, and low iron (11–15). Capsule formation is also increased by excess of calcium in minimal medium (16), suggesting the existence of a nonenzymatic process of enlargement involving ionic cross-linking and aggregation of PS molecules. Two not mutually exclusive models of capsule enlargement have been suggested: (i) proximal growth, in which addition of new PS is incorporated in the cell surface, displacing preexisting molecules to the outer edge (17); and (ii) distal growth, where addition of new PS is incorporated at the capsule edge (18). Regardless of the directionality of capsule growth or the assembly process, an increase in capsule size appears to result from the synthesis and incorporation of new PS molecules of increasing dimensions (19, 20).

Visual monitoring of capsule growth is challenging due to the capsule's high water content (~99% [vol/vol]) (21), which contributes to a small refractive index difference in aqueous solutions that precludes observation by simple light microscopy. Furthermore, the hydration of the PS capsule makes it susceptible to dehydration procedures, which essentially precludes ultrastructural studies using electron microscopy (22). Scanning electron and confocal microscopy techniques can be used to visualize capsular material in whole cryptococcal yeast cells, with the latter exploiting fluorescently labeled antibodies (Abs) to GXM (10, 17, 23–26). In addition, capsule visualization can also be achieved by light microscopy (i) through negative staining of yeast cells by suspension in India ink or (ii) by the capsular reaction ("quellung" reaction) that follows binding of Abs to GXM (27–29). India ink particles allow visualization through their exclusion by the capsule,

Received 17 July 2013 **Accepted** 11 August 2013

Published ahead of print 16 August 2013

Address correspondence to Arturo Casadevall, arturo.casadevall@einstein.yu.edu.

* Present address: Radames J. B. Cordero, Programa de Pós Graduação em Química Biológica, Instituto de Bioquímica Médica and Instituto de Microbiologia, Universidade Federal do Rio de Janeiro, Rio de Janeiro, Brazil.

Supplemental material for this article may be found at http://dx.doi.org/10.1128/EC.00163-13.

doi:10.1128/EC.00163-13

whereas the binding of capsular Abs allows visualization of the capsule by altering capsular optical properties such that the capsule can be distinguished from the surrounding aqueous medium.

In this study, we present the first temporal behavior analysis of capsule enlargement from 10 different *C. neoformans* H99 cells grown *in vitro* under capsule-inducing conditions. The capsule was labeled with monoclonal antibody (MAb) 13F1, an IgM that changes the optical properties of the capsule without significantly altering its elastic properties (30). This method allowed us to study capsule and cell body volume increase as a function of time, and the data provide new insight into the process of *C. neoformans* capsule synthesis, assembly, and architecture.

MATERIALS AND METHODS

C. neoformans serotype A strain H99 (ATCC 208821) cells from frozen stock were grown overnight in Sabouraud rich medium at 30°C under constant agitation. One milliliter of yeast cells was washed 3 times with phosphate-buffered saline (PBS) and enumerated using a hemocytometer. Approximately 10^4 cells were placed in a Lab-Tek chambered cover glass (Thermo Fisher Scientific, Rochester, NY) containing 200 μl of minimal medium containing 125 mM mannitol, 10 mM $MgSO_4$, 29.3 mM KH_2PO_4, 13 mM glycine, and 3 μM thiamine-HCl (adjusted to pH 5.5 and 37°C) (12), supplemented with 20 μg/ml of IgM MAb 13F1 (31). This MAb was purified from hybridoma cell supernatant recovered after 14 days of growth using UltraLink immobilized-mannan binding protein (Pierce, Rockford, IL) chromatography.

The chamber slide was placed in a temperature-controlled microscope chamber adjusted to 37°C 2 h prior to recording. Image acquisition was done at 5-min intervals and different z-focus distances with a 63× differential interference contrast (DIC) objective in an Axiovert 200 M inverted microscope equipped with a Hamamatsu ORCA ER cooled charge-coupled device (CCD) camera and controlled by Axio Vision 4.6 software (Carl Zeiss Micro Imaging, New York, NY).

The whole-cell radius and cell body radius (r_c and r_b, respectively) were determined from time-lapse microscopy images using ImageJ software (National Institutes of Health, Bethesda, MD). For each cell, approximately 20 frames (20-min interval for a total of 400 min) were analyzed, with 3 line measurements (vertical, horizontal, and diagonal) across the whole cell (capsule included) and across cell body dimensions. The capsule average volume ($V_{capsule}$) was calculated by subtracting the volume of the whole cell, V_{cell} ($4/3\ \pi\ r_c^3$), from that of the cell body, V_{body} ($4/3\ \pi\ r_b^3$). Capsule and cell body growth curves (volume increase as a function of time) were fitted to different growth model equations (variable slope sigmoidal, Gompertz, logistic, and Weibull) using GraphPad Prism, version 5.0b (GraphPad Software, San Diego, CA). The Akaike's information criterion (AIC) method was used to determine the best model. Linear portions of curves were fitted to linear regression analysis to determine capsule and cell body growth rate (slope). Determination of capsule and cell body differences in radii, modeling, and calculations for the parameter alpha were done using MATLAB.

RESULTS

C. neoformans dimensions were recorded and measured over a period of 400 min for 10 individual cells. Both capsule enlargement and cell body enlargement could be simultaneously observed (see Movie S1 in the supplemental material). The halo depicting the outer edge of the PS capsule resulting from the "quellung" effect of MAb 13F1 (IgM) displaced away from the cell body as a function of time. Capsule growth appeared to be a continuous process with homogeneous circumferential enlargement. A cell was identified as dead by a quiescent cytoplasm devoid of any organelle motion. The dead cell manifested no capsule and/or cell growth and served as a negative control (see Movie S1).

Capsule growth as a function of time followed a nonlinear behavior, and we observed considerable cell-to-cell variation in the temporal kinetics of capsule and cell body growth (Fig. 1A). The growth curves were fitted to sigmoidal (4-parameter), Gompertz, Weibull, and logistic exponential equations, the latter being the most likely to be correct based on the Akaike's information criterion method (32) (Table 1). Capsules enlarged approximately from 3 to 15 times their initial volume sizes (y_{max}/y_{min}) and exhibited similar k values around 0.01 min (Table 2). Consistent with a logistic growth model, the final capsule size showed a positive and significant correlation with growth rate (slope of the curve, g) (Fig. 1A). The increase of cell body volume per unit of time did not show good fittings to a logistic growth model (Table 2), and the final cell body size did not correlate with the rate of its growth (Fig. 1B). These results suggest that the capsule and cell body follow distinct growth mechanisms and/or distinct time scales for their biosynthesis.

On average, most of the capsule enlargement (~70%) occurred prior to the first cellular replication event, when it switched from linear growth to a steady state (Fig. 1A). Some cells, however, continued to show some capsule growth during replication. The budding time varied between each replication event and among cells (Fig. 1A), consistent with previous reports (30). We noted that replication of *C. neoformans* cells occurred after attainment of a critical cell body size, ranging from 5 to 6 μm in diameter.

Linear regression analysis of exponential portions demonstrated that capsules always grew faster than the cell body ($P = 0.004$ based on paired t test), which is at least 4-fold faster (Table 3). The increase in capsule radius per unit of time was directly proportional and/or controlled by a single parameter (alpha), representing the relative growth rate of capsule to cell body. When the ratio is above 1/2, the capsule radius monotonically diverges from the cell boundaries. However, reduction of alpha below 1/2 results in an initial drop in the difference between the capsule and cell body radii followed by an exponential growth difference (Fig. 1C). The difference in radii of capsule and cell body for all cells demonstrated that the capsule envelope is monotonically increasing, or escaping the cellular boundaries, at least twice as fast the rate of cell body growth (Fig. 1D). Together, these results suggest that the size of growth of the capsule is dependent on the rate of its biosynthesis and suggest both a window of opportunity for capsule buildup preceding cellular replication and a minimum growth rate in order to escape the spherical volume boundaries of the cell body.

DISCUSSION

Capsule synthesis is an important adaptation mechanism for several pathogens that cause infection and disease. In *C. neoformans*, capsular enlargement appears to be a survival strategy that occurs in response to predatory amoebae and during mammalian infection (4). Cryptococcal capsular enlargement implies an orchestrated array of biochemical processes and substantial energy investment, considering its complex composition and large dimensions.

The understanding of capsule construction is hampered by the capsule's complex molecular structure (4) and high water content (21) and the limited methodology for its study. Therefore, any effort at visualization and direct analysis of capsule growth has to overcome the capsule's fragility and dynamics. Furthermore,

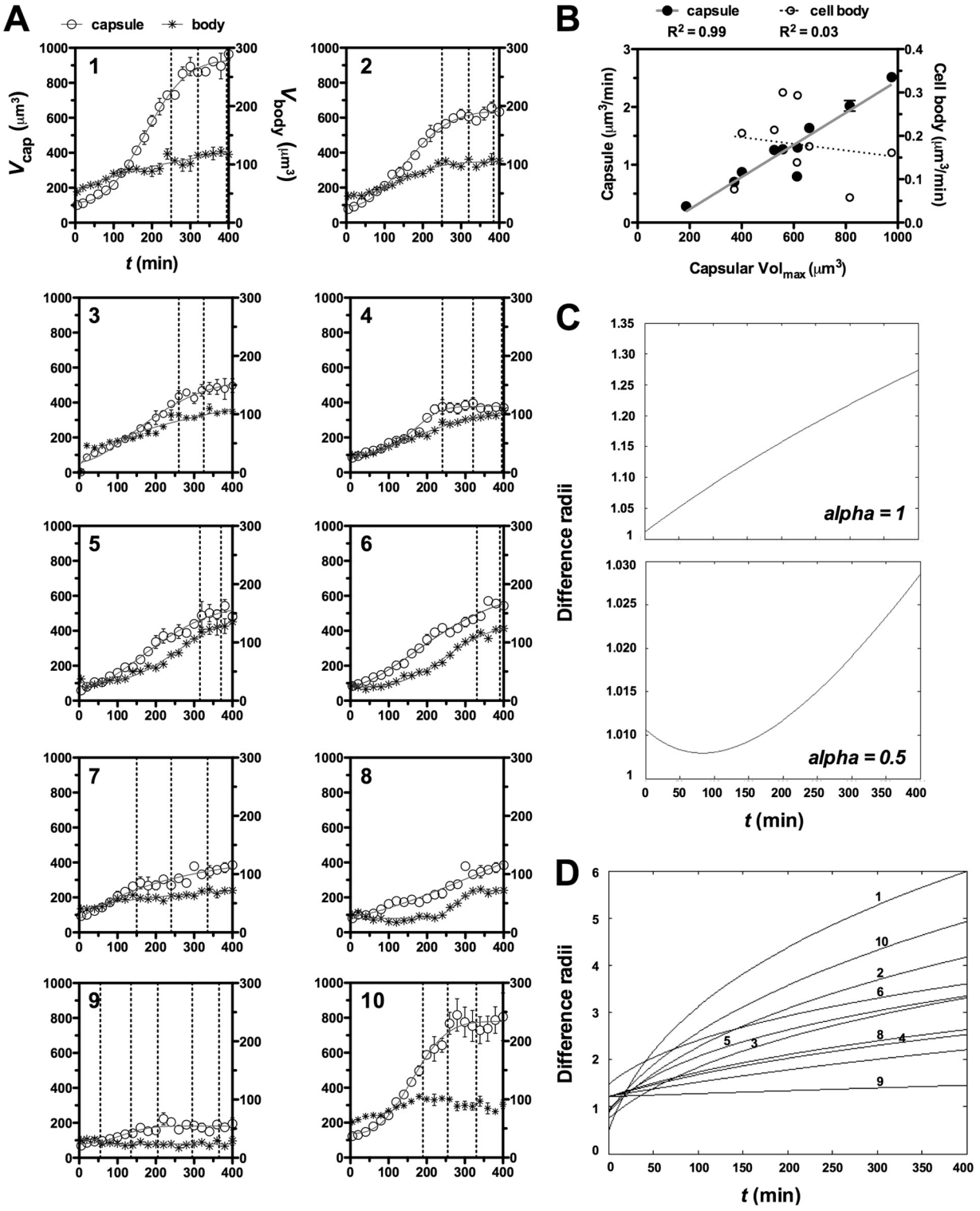

FIG 1 (A) Increase of capsule and cell body volume as a function of time. Capsule and cell body dimensions of 10 different *C. neoformans* H99 cells (each panel is a different cell) are expressed as volume (capsule, open circles; cell body, stars). Data points represent average values of three size measurements ± standard deviations and were fitted using a logistic growth function equation. Vertical lines on *x* axes indicate the occurrence of a budding event during period of analysis (400 min). (B) Capsule final size correlates positively with capsule growth rate. Linear regression analysis between final capsule volumes (*x* axes) and capsule growth rates (left *y* axes, filled circles) showed a significant ($R^2 = 0.99$, $P < 0.001$) correlation between rate and final capsule size. A lack of correlation was observed compared to cell body growth rate ($R^2 = 0.03$, $P = 0.7$) (right *y* axes, open circles). (C) Capsule growth is affected by one parameter, alpha. (D) Monotonic increase of capsule relative to cell body for each cell, with the numbers corresponding to the panels for individual cells shown in panel A.

TABLE 1 Comparison of different growth model equations for data analysis of capsule volume as a function of time based on the AIC method[a]

Cell	AIC value by equation			
	Sigmoidal[b]	Gompertz[c]	Logistic[d]	Weibull[e]
1	4,686.4	6,339.5	*3,246.9*	3,519.1
2	4,526.3	3,777.8	*2,370.2*	2,909.5
3	10,780.9	5,052.5	*3,235.6*	6,507.5
4	3,065.8	4,005.6	2,744.9	*2,138.5*
5	10,110.5	6,818.3	*3,864.3*	6,527.1
6	13,366.4	7,068.9	*3,764.9*	9,256.2
7	14,473.0	3,745.8	*3,130.7*	16,689.4
8	18,695.9	72,989.9	*14,740.3*	2,043.3
9	*3,385.3*	6,818.3	3,864.3	6,527.1
10	7,006.7	7,124.1	*4,653.7*	4,845.9

[a] For details, see reference 32. Based on the AIC model, the equation with the smallest AIC value (showed in italic type) is most likely to be correct.

[b] The sigmoidal growth equation is $Y = Y_{min} + \frac{Y_{max} - Y_{min}}{1+10^{(\log k - x)g}}$, where y_{max} and y_{min} are the maximum and initial volumes, respectively, k is the value of x at halfway between y_{min} and y_{max}, and g is the slope.

[c] The Gombertz growth equation is $Y = Y_{max}\, e^{(\ln Y_{min}/Y_{max})e^{-kx}}$.

[d] The logistic growth equation is $Y = \frac{Y_{max} \times Y_{min}}{(Y_{max} - Y_{min})e^{-kt} + Y_{min}}$.

[e] The Weibull growth equation is $Y = Y_{max} - (Y_{max} - Y_{min})e^{-1(kt)^g}$.

TABLE 3 Rate of capsule and cell body volume increase[a]

Cell	Increase in vol (μm^3/min) of:		Fold change (capsule/cell body)
	Capsule	Cell body	
1	2.51 ± 0.07	0.16 ± 0.01	15.7
2	1.63 ± 0.05	0.18 ± 0.01	9.1
3	1.25 ± 0.04	0.21 ± 0.01	6.0
4	0.87 ± 0.04	0.21 ± 0.01	4.1
5	1.27 ± 0.04	0.30 ± 0.01	4.2
6	1.30 ± 0.03	0.29 ± 0.01	4.5
7	0.70 ± 0.03	0.07 ± 0.01	10.0
8	0.80 ± 0.03	0.14 ± 0.01	5.7
9	0.28 ± 0.03		
10	2.02 ± 0.09	0.06 ± 0.01	33.7

[a] Growth rate (μm^3/min) was determined by linear regression analysis of capsule or cell body radial length increase (μm^3) as a function of time (min). Regression analysis was performed on the first 100 or 200 min of imaging, previous to the beginning of cellular replication.

there is also the concern that any method used to visualize the capsule could affect the process of capsule growth.

In a prior study, we were able to identify the utility of MAb 13F1 for probing capsule enlargement. Although this MAb does change the refractive index of the capsule and allows visualization by light microscopy, it has little or no effect on the mechanical properties of the capsule (30). Consequently, MAb 13F1 labeling provides the first means to study capsule growth dynamics in real time. Here we report the first temporal analysis of H99 *C. neoformans* capsule and cell body enlargement using time-lapse microscopy and present an updated view for capsule synthesis, architecture, and assembly.

Our kinetic analysis revealed that capsule enlargement follows a logistic growth model. This type of exponential growth has been associated with autocatalytic reactions in which products can also act as reagents, resulting in spontaneous order and cooperativity. This finding is consistent with our prior observation that PS molecules carry structural information for capsule self-assembly (16, 33). In addition, the observed nonlinear growth demonstrates that the final capsule size is proportional to the rate of its growth (slope of curve). This suggests that the capsule dimensions are regulated by the rate of biosynthesis of its building blocks and the existence of a window of opportunity for capsule growth that may be related to the mitotic cycle.

The poor goodness of fit observed with the cell body volume increase per unit of time suggests that capsule and cell body enlargement follow distinct growth mechanisms and/or that they occur at different time scales. It is possible that this growth rate difference might reflect a metabolic priority toward the biosynthesis of capsular over cell wall building blocks. Alternatively, rather than focusing the anabolic activity toward a particular structure, the capsule could appear to grow faster as a consequence of the density and spatial organization between its components relative to the cell body structure.

We noted a relationship between capsule enlargement and cell division. For most cells, there was significant and simultaneous growth of the capsule and cell body previous to the first replication event. This relationship suggests that, like the cell body growth (34), capsule enlargement could represent a coordinated group of processes linked to the cell cycle. The observation that capsule enlargement was the first sign of metabolic activity demonstrates that *C. neoformans* prioritizes enlarging its capsule rather than its replication. Although the capsule is not required for *C. neofor-*

TABLE 2 Capsule and cell volume increase as a function of time[a]

Cell	y_{max} (μm^3)		y_{min} (μm^3)		k (min)		R^2	
	Capsule	Body	Capsule	Body	Capsule	Body	Capsule	Body
1	976.3 ± 15.6	138.9 ± 9.3	64.6 ± 5.6	58.4 ± 2.1	0.015 ± 0.0006	0.006 ± 0.001	0.99	0.86
2	659.9 ± 9.6	112.8 ± 3.4	63.8 ± 5.5	38.4 ± 2.0	0.015 ± 0.0006	0.009 ± 0.001	0.98	0.93
3	539.3 ± 16.2	130.3 ± 9.9	66.1 ± 6.0	35.8 ± 2.0	0.012 ± 0.0008	0.007 ± 0.001	0.97	0.92
4	401.1 ± 10.5	116.6 ± 4.5	61.4 ± 6.9	25.3 ± 1.2	0.014 ± 0.0012	0.008 ± 0.001	0.93	0.97
5	558.1 ± 19.9	237.9 ± 39.9	61.9 ± 6.3	21.1 ± 1.7	0.012 ± 0.0008	0.007 ± 0.001	0.96	0.96
6	614.6 ± 20.3	176.5 ± 14.3	78.8 ± 5.4	14.3 ± 1.2	0.010 ± 0.0006	0.009 ± 0.001	0.98	0.97
7	371.5 ± 12.1	73.7 ± 3.6	94.4 ± 8.4	39.7 ± 1.8	0.011 ± 0.0012	0.007 ± 0.002	0.91	0.78
8	612.3 ± 106.4	92.8 ± 10.2	85.3 ± 6.4	3.9 ± 1.2	0.006 ± 0.0008	0.012 ± 0.002	0.94	0.91
9	186.6 ± 5.8	24.1 ± 0.8	62.6 ± 7.8	33.4 ± 2.8	0.015 ± 0.0025	0.019 ± 0.011	0.75	0.24
10	815.2 ± 20.7	93.8 ± 1.6	73.9 ± 11.2	55.6 ± 3.9	0.016 ± 0.0013	0.018 ± 0.004	0.95	0.63

[a] Data were fitted using a logistic (3-parameter) nonlinear exponential equation.

mans viability, since acapsular mutants are viable (34, 35), the prioritization of capsule biosynthesis could reflect the importance of this surface modification for cryptococcal biology. In this regard, we note that the capsule is likely to serve a critical protective function during both mammalian infection and environmental survival, given that it protects against phagocytic cells and predators (36).

The rate and temporal behavior of capsule growth varied considerably among cells. This difference could account for the heterogeneity in capsule size observed in encapsulated cryptococcal samples. The rate of capsule enlargement was at least 4-fold faster than that of the cell body. It appears that the capsule must grow at least one-half as fast as the cell body to escape the boundaries depicted by the cell body envelope. Based on our measurement, *C. neoformans* cell body growth appears to occur approximately 100-fold slower than that reported for *Saccharomyces cerevisiae* (37).

The outward displacement of the capsule edge delineated by the "quellung" effect suggests a capsule growth model that includes proximal incorporation (at the cell body surface) of new PS molecules, displacing preexisting ones to the outer surface, as suggested previously (17). This, however, does not rule out the existence of simultaneous capsule growth by apical extension (18). A capsule in a growth model consisting solely of addition of new PS molecules at the capsule distal site (edge) would, in theory, be expected to exhibit a lower growth rate as a function of capsule size or, as the distance from the capsule edge to cell body increases, if the biosynthetic process was constant as a function of time and the density of capsular material was constant as a function of capsule radius. However, the density of capsular PS is known to decrease in the outer regions (24, 38), and the apical extension model could yield exponential growth if assembly of a less-dense outer capsule required less biosynthetic capacity than denser interior regions. Hence, nonlinear kinetics could be accommodated by either the proximal or apical extension models, and given that these are not mutually exclusive, we prefer a capsule growth model that includes PS addition at both distal and proximal capsule sites, since such a model would allow incorporation and reconciliation of all previous data (17, 18).

In summary, we provide the first cinematographic demonstration of capsular enlargement and cell body growth. Our results show great cell-to-cell variation in the temporal kinetics of capsule and cell body growth. Analysis of the rate of capsule growth can be reconciled with models of either proximal or apical growth. Overall, our results provide evidence that capsule growth follows an exponential growth pattern and is a highly regulated process that is linked to the timing of cell cycle progression.

ACKNOWLEDGMENTS

This work was supported by the National Institutes of Health grants AI033774, HL059842, and AI033142 to A.C. and R.J.B.C. R.J.B.C. was supported by grant T32 AI7506-15. R.J.B.C. is currently supported by CAPES/Programa Ciências sem Fronteiras.

We thank Nathan B. Viana for valuable discussion, all members of the A.C. lab who have worked on the problem of capsule growth visualization, and Antonio S. Nakouzi for purifying and providing MAb 13F1.

REFERENCES

1. **Del Poeta M.** 2004. Role of phagocytosis in the virulence of Cryptococcus neoformans. Eukaryot. Cell **3:**1067–1075.
2. **O'Meara TR, Alspaugh JA.** 2012. The Cryptococcus neoformans capsule: a sword and a shield. Clin. Microbiol. Rev. **25:**387–408.
3. **Feldmesser M, Kress Y, Casadevall A.** 2001. Dynamic changes in the morphology of Cryptococcus neoformans during murine pulmonary infection. Microbiology **147:**2355–2365.
4. **Zaragoza O, Rodrigues ML, De Jesus M, Frases S, Dadachova E, Casadevall A.** 2009. The capsule of the fungal pathogen Cryptococcus neoformans. Adv. Appl. Microbiol. **68:**133–216.
5. **Cherniak R, Valafar H, Morris LC, Valafar F.** 1998. Cryptococcus neoformans chemotyping by quantitative analysis of 1H nuclear magnetic resonance spectra of glucuronoxylomannans with a computer-simulated artificial neural network. Clin. Diagn. Lab. Immunol. **5:**146–159.
6. **Garcia-Rivera J, Chang YC, Kwon-Chung KJ, Casadevall A.** 2004. Cryptococcus neoformans CAP59 (or Cap59p) is involved in the extracellular trafficking of capsular glucuronoxylomannan. Eukaryot. Cell **3:**385–392.
7. **Rodrigues ML, Nimrichter L, Oliveira DL, Frases S, Miranda K, Zaragoza O, Alvarez M, Nakouzi A, Feldmesser M, Casadevall A.** 2007. Vesicular polysaccharide export in Cryptococcus neoformans is a eukaryotic solution to the problem of fungal trans-cell wall transport. Eukaryot. Cell **6:**48–59.
8. **Yoneda A, Doering TL.** 2006. A eukaryotic capsular polysaccharide is synthesized intracellularly and secreted via exocytosis. Mol. Biol. Cell **17:**5131–5140.
9. **Reese AJ, Doering TL.** 2003. Cell wall alpha-1,3-glucan is required to anchor the Cryptococcus neoformans capsule. Mol. Microbiol. **50:**1401–1409.
10. **Rodrigues ML, Alvarez M, Fonseca FL, Casadevall A.** 2008. Binding of the wheat germ lectin to Cryptococcus neoformans suggests an association of chitinlike structures with yeast budding and capsular glucuronoxylomannan. Eukaryot. Cell **7:**602–609.
11. **Granger DL, Perfect JR, Durack DT.** 1985. Virulence of Cryptococcus neoformans. Regulation of capsule synthesis by carbon dioxide. J. Clin. Invest. **76:**508–516.
12. **Guimaraes AJ, Frases S, Cordero RJ, Nimrichter L, Casadevall A, Nosanchuk JD.** 2010. Cryptococcus neoformans responds to mannitol by increasing capsule size in vitro and in vivo. Cell. Microbiol. **12:**740–753.
13. **Vartivarian SE, Anaissie EJ, Cowart RE, Sprigg HA, Tingler MJ, Jacobson ES.** 1993. Regulation of cryptococcal capsular polysaccharide by iron. J. Infect. Dis. **167:**186–190.
14. **Zaragoza O, Casadevall A.** 2004. Experimental modulation of capsule size in Cryptococcus neoformans. Biol. Proced. Online **6:**10–15.
15. **Zaragoza O, Fries BC, Casadevall A.** 2003. Induction of capsule growth in Cryptococcus neoformans by mammalian serum and CO_2. Infect. Immun. **71:**6155–6164.
16. **Nimrichter L, Frases S, Cinelli LP, Viana NB, Nakouzi A, Travassos LR, Casadevall A, Rodrigues ML.** 2007. Self-aggregation of Cryptococcus neoformans capsular glucuronoxylomannan is dependent on divalent cations. Eukaryot. Cell **6:**1400–1410.
17. **Pierini LM, Doering TL.** 2001. Spatial and temporal sequence of capsule construction in Cryptococcus neoformans. Mol. Microbiol. **41:**105–115.
18. **Zaragoza O, Telzak A, Bryan RA, Dadachova E, Casadevall A.** 2006. The polysaccharide capsule of the pathogenic fungus Cryptococcus neoformans enlarges by distal growth and is rearranged during budding. Mol. Microbiol. **59:**67–83.
19. **Frases S, Pontes B, Nimrichter L, Viana NB, Rodrigues ML, Casadevall A.** 2009. Capsule of Cryptococcus neoformans grows by enlargement of polysaccharide molecules. Proc. Natl. Acad. Sci. U. S. A. **106:**1228–1233.
20. **Yoneda A, Doering TL.** 2008. Regulation of Cryptococcus neoformans capsule size is mediated at the polymer level. Eukaryot. Cell **7:**546–549.
21. **Maxson ME, Cook E, Casadevall A, Zaragoza O.** 2007. The volume and hydration of the Cryptococcus neoformans polysaccharide capsule. Fungal Genet. Biol. **44:**180–186.
22. **Cleare W, Casadevall A.** 1999. Scanning electron microscopy of encapsulated and non-encapsulated Cryptococcus neoformans and the effect of glucose on capsular polysaccharide release. Med. Mycol. **37:**235–243.
23. **Araujo GS, Fonseca FL, Pontes B, Torres A, Cordero RJB, Zancopé-Oliveira RM, Casadevall A, Viana NB, Nimrichter L, Rodrigues ML, Garcia ES, de Souza W, Frases S.** 2012. Capsules from pathogenic and non-pathogenic Cryptococcus spp. manifest significant differences in structure and ability to protect against phagocytic cells. PLoS One **7:**e29561. doi:10.1371/journal.pone.0029561.
24. **Gates MA, Thorkildson P, Kozel TR.** 2004. Molecular architecture of the Cryptococcus neoformans capsule. Mol. Microbiol. **52:**13–24.
25. **Maxson ME, Dadachova E, Casadevall A, Zaragoza O.** 2007. Radial mass

density, charge, and epitope distribution in the Cryptococcus neoformans capsule. Eukaryot. Cell **6:**95–109.
26. **Mershon-Shier KL, Vasuthasawat A, Takahashi K, Morrison SL, Beenhouwer DO.** 2011. In vitro C3 deposition on Cryptococcus capsule occurs via multiple complement activation pathways. Mol. Immunol. **48:**2009–2018.
27. **MacGill TC, MacGill RS, Casadevall A, Kozel TR.** 2000. Biological correlates of capsular (quellung) reactions of Cryptococcus neoformans. J. Immunol. **164:**4835–4842.
28. **Mukherjee J, Cleare W, Casadevall A.** 1995. Monoclonal antibody mediated capsular reactions (Quellung) in Cryptococcus neoformans. J. Immunol. Methods **184:**139–143.
29. **Neufeld F.** 1902. Über die Agglutination der Pneumokokken und über die Theorien der Agglutination. Z. Hyg. Infektionskr. **40:**54–72.
30. **Cordero RJ, Pontes B, Frases S, Nakouzi AS, Nimrichter L, Rodrigues ML, Viana NB, Casadevall A.** 2013. Antibody binding to Cryptococcus neoformans impairs budding by altering capsular mechanical properties. J. Immunol. **190:**317–323.
31. **Mukherjee J, Casadevall A, Scharff MD.** 1993. Molecular characterization of the humoral responses to Cryptococcus neoformans infection and glucuronoxylomannan-tetanus toxoid conjugate immunization. J. Exp. Med. **177:**1105–1116.
32. **Motulsky HJ, Christopoulos A.** 2003. Fitting models to biological data using linear and nonlinear regression. A practical guide to curve fitting. GraphPad Software, Inc, San Diego, CA.
33. **McFadden DC, De Jesus M, Casadevall A.** 2006. The physical properties of the capsular polysaccharides from Cryptococcus neoformans suggest features for capsule construction. J. Biol. Chem. **281:**1868–1875.
34. **Fromtling RA, Shadomy HJ, Jacobson ES.** 1982. Decreased virulence in stable, acapsular mutants of Cryptococcus neoformans. Mycopathologia **79:**23–29.
35. **Chang YC, Kwon-Chung KJ.** 1994. Complementation of a capsule-deficient mutation of Cryptococcus neoformans restores its virulence. Mol. Cell. Biol. **14:**4912–4919.
36. **Zaragoza O, Chrisman CJ, Castelli MV, Frases S, Cuenca-Estrella M, Rodriguez-Tudela JL, Casadevall A.** 2008. Capsule enlargement in Cryptococcus neoformans confers resistance to oxidative stress suggesting a mechanism for intracellular survival. Cell. Microbiol. **10:**2043–2057.
37. **Sun J, Stowers CC, Boczko EM, Li D.** 2010. Measurement of the volume growth rate of single budding yeast with the MOSFET-based microfluidic Coulter counter. Lab Chip **10:**2986–2993.
38. **Bryan RA, Zaragoza O, Zhang T, Ortiz G, Casadevall A, Dadachova E.** 2005. Radiological studies reveal radial differences in the architecture of the polysaccharide capsule of Cryptococcus neoformans. Eukaryot. Cell **4:**465–475.